European Journal of Public Health Studies
ISSN: 2668 - 1056
ISSN-L:2668 - 1056
Available on-line at: www.oapub.org/hlt

DOI: 10.46827/ejphs.v9i2.274 Volume 9 | Issue 2 | 2026

BISDEMETHOXYCURCUMIN ATTENUATES SCIATIC NERVE INJURY IN VINCRISTINE- INDUCED NEUROPATHIC PAIN MICE[i]

Chalton Manengu[ii]
College of Pharmacy,
Ningxia Medical University,
1160 Shengli Street,
Yinchuan 750004,
Ningxia Hui Autonomous Region,
China
College of Pharmaceutical Sciences,
Southwest University,
Tiansheng Road Beibei District,
Chongqing 400715,
China

Abstract:
Chemotherapy-induced neuropathic pain is a common side effect for cancer patients. There are many therapeutic choices available today, but they typically have negative side effects and are ineffective at reducing pain. As a result, novel strategies for treating chemotherapy induced neuropathic pain are being investigated, particularly those involving natural substances. Bisdemethoxycurcumin (BDCM), a component of turmeric, is a potential target. This study explores the potential of BDCM in lessening pain sensitivity and restoring sciatic nerve damage. Mice were injected with vincristine sulfate intraperitoneally to create the study model. The cold plate test, thermal radiation test, and Von Frey test were used to evaluate the potential pain-relieving benefits of BDCM. We employed transmission electron microscopy (TEM), hematoxylin and eosin staining, silver staining, and an electrophysiological stimulation test to assess BDCM's possible neuroprotective effect on the sciatic nerve. We further evaluated BDCM's effects on NF-κB and pro-inflammatory cytokines. BDCM treatment reduced the frequency of paw lifts, increased the latency before paw withdrawal, and significantly raised the paw withdrawal threshold. BDCM reduced sciatic nerve tissue damage and increased sensory nerve conduction velocity. Additionally, BDCM decreased NF-κB and pro-inflammatory cytokines expression. These findings demonstrate that BDCM alleviates VCR-induced sciatic nerve damage and preserves nerve integrity, highlighting its potential as a novel therapeutic agent for neuropathic pain and further studies should further explore its mechanisms in neuropathic pain attenuation.

[i] 去甲氧基姜黄素减轻长春新碱诱导的神经性疼痛小鼠坐骨神经损伤
[ii] Correspondence: email chaltonmanengu179@gmail.com

Keywords: bisdemethoxycurcumin; vincristine; chemotherapy; neuropathic pain; antinociception; neuroprotection

摘要:
化疗诱导的神经性疼痛是癌症患者常见的不良反应。目前已有多种治疗选择，但通常存在副作用且在缓解疼痛方面疗效有限。因此，研究者正在探索新的治疗策略，尤其是基于天然物质的干预方法。去甲氧基姜黄素（BDCM）是姜黄中的一种成分，具有潜在的治疗价值。本研究探讨 BDCM 在降低痛觉敏感性和修复坐骨神经损伤方面的作用。通过腹腔注射硫酸长春新碱建立小鼠模型。采用冷板实验、热辐射实验和 Von Frey 实验评估 BDCM 的镇痛效果。通过透射电子显微镜（TEM）、苏木精-伊红染色、银染以及电生理刺激实验评估 BDCM 对坐骨神经的神经保护作用。同时检测 BDCM 对 NF-κB 及促炎细胞因子的影响。BDCM 处理降低了小鼠抬足频率，延长了足部撤回潜伏期，并显著提高了足部撤回阈值。BDCM 减轻了坐骨神经组织损伤，并提高了感觉神经传导速度。此外，BDCM 降低了 NF-κB 及促炎细胞因子的表达。这些结果表明，BDCM 可缓解长春新碱诱导的坐骨神经损伤并维持神经结构完整性，提示其作为治疗神经性疼痛的新型药物具有潜在价值，后续研究应进一步阐明其在缓解神经性疼痛中的作用机制。

关键词: 去甲氧基姜黄素；长春新碱；化疗；神经性疼痛；镇痛作用；神经保护作用

1. Introduction

Chemotherapeutic drugs can induce prolonged pain and nerve damage, which is known as chemotherapy-induced neuropathic pain (CINP) [1, 2]. Patients' quality of life is negatively impacted by this illness, which results in psychological stress, functional limits, physical discomfort, and decreased treatment compliance [3]. 20–50% of individuals taking typical chemotherapy regimens may develop CINP, though prevalence varies depending on the particular medications and dosages given [4]. The symptoms, which frequently result in severe agony, range from tingling and numbness to acute, scorching pain. Degeneration of sensory neurons, demyelination of nerve fibers, and decreased epidermal nerve fiber density are all linked to CINP. A chronic condition of pain is thought to result from altered pain signaling caused by changes in axonal structure [5].

Neuropathic pain is caused by various molecular pathways, including activation of nuclear factor-kappa B (NF-κB). NF-κB is a transcription factor that affects physiological activities such inflammation, immunological responses, and pain signaling [6, 7]. It increases pain receptor sensitivity, speeds up pain transmission in the sciatic nerve and spinal cord, and stimulates the release of pain-related neurotransmitters [8, 9]. NF-κB may play a substantial role in neuropathic pain start and persistence [10]. Nerve

damage or hypersensitivity triggers a sequence of events that activate NF-κB. NF-κB activation leads to increased production of pro-inflammatory cytokines like IL-1β, IL-6, and TNF-α, worsening chronic pain associated with neuropathic disorders [11, 12]. To treat neuropathic pain, blocking or modifying NF-κB activation may reduce inflammation, dampen pain signals, and alleviate symptoms.

Standard therapies for neuropathic pain are frequently limited by serious side effects. In contrast, BDCM, a natural curcuminoid produced from the popular spice turmeric (*figure 1*) [13, 14], has shown anti-inflammatory, antioxidant, and anticancer activity in multiple preclinical studies. BDCM has been demonstrated to affect a variety of inflammatory pathways [15]. It reduces the production of inflammatory cytokines such IL-6, IL-1β, and TNF-α by reducing NF-κB activation and IκB degradation [16], potentially aiding in pain alleviation. It lowers inducible NF-κB in Raw 264.7 macrophages and reduces carrageenan-induced paw edema in mice [17]. Consequently, this study proposes that BDCM will produce pain-relieving and nerve-protecting effects in a mouse model of vincristine-induced neuropathic pain through the specific inhibition of the NF-κB signaling pathway.

2. Methods

2.1 Animals

Adult male ICR mice weighing between 18 and 22g were used in the investigation. These mice, which have the certification number SCXK Ningxia 2020-0001, were obtained from Ningxia Medical University's experimental animal center. The animals were kept in plastic cages with a 12-hour light/dark cycle at a controlled temperature of 25 °C ± 2 °C. Water and a standard laboratory diet were freely available. The Ningxia Medical University Animal Ethics Committee approved all animal-related procedures.

2.1.1 Experimental Animal Model

The experimental model was established by inducing neuropathic pain in mice. This was achieved through once-daily intraperitoneal injections of vincristine sulfate at a dosage of 75μg/kg for 10 consecutive days, following established methods [18, 19]. The vincristine sulfate was sourced from Guangdong Lingnan Pharmaceutical Co., Ltd, with the batch number 667016.

2.2 Drugs

Male ICR mice were allocated into six groups, each containing 10 animals. The groups were defined as follows: (i) Control group: mice received saline for 21 days. (ii) VCR + Saline group: mice were administered vincristine sulfate (VCR; 75 μg/kg, i.p.) daily for 10 days, followed by normal saline for the subsequent 11 days. (iii) Three VCR + BDCM groups: after 10 days of VCR administration, mice received oral BDCM at doses of 20, 40, or 80 mg/kg daily for 11 days. (iv) VCR + Pregabalin group: following the 10-day VCR

regimen, mice were treated with pregabalin (10 mg/kg, i.p.) for 11 days. All dosages were selected based on previous research [1-5].

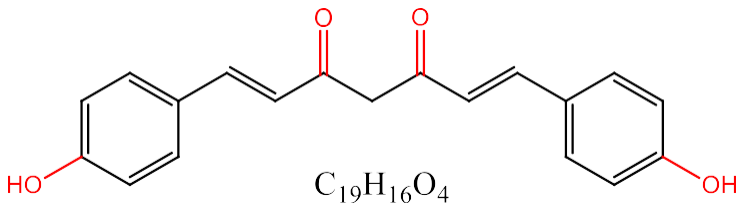

Bisdemethoxycucurmin
(BDCM)

Figure 1: Chemical structure of Bisdemethoxycurcumin (BDCM)

2.3 Behavioral tests

2.3.1 Von Frey filament test

Mechanical nociception, which gauges an animal's sensitivity to a painful stimulus, was assessed using the Von Frey filament test. The paw withdrawal threshold (PWT) was assessed using the up-and-down approach outlined by Chaplan et al. (1994) [20]. The mid-plantar region of the hind paw was accessible by placing each mouse separately in a transparent Plexiglas container with a wire mesh floor. They were placed in a quiet, dim lighted room and given time to become used to this setting. The mid-plantar surface was then subjected to a series of calibrated Von Frey filaments applied perpendicularly, starting with a filament applying 0.16g of force. After gently pressing each filament until it bent, it was held in place for two to three seconds. The testing was done in the following order: the next stronger filament was used if there was no response, and the next weaker filament was used if there was a positive response (like paw withdrawal, licking, or shaking). This up-and-down pattern persisted until six to ten measurements were taken.

2.3.2 Thermal radiation test

To determine the paw withdrawal latency (PWL), the heat radiation test was conducted using the procedure outlined by Hargreaves et al. (1988) [21]. Mice were placed inside transparent glass enclosures on a platform made of clear glass. Then, from underneath the glass, a radiant heat source was directed onto the plantar surface of a hind paw. With a 20-second cutoff to avoid tissue damage, the duration until a nocifensive reaction such as lifting, licking, or shaking the paw was noted. At least three measurements were made during each test session, with the heat stimulus being administered every five minutes [22].

2.3.3 Cold-plate test

According to Jasmin et al. (1998) [23], the cold plate test was used to measure sensitivity to a non-painful cold stimulus, specifically cold allodynia. In this process, mice were kept at 4.0 ± 0.5°C in a clear Plexiglas container on a metal plate. The number of hind paw lifts,

licks, or shakes was counted during a five-minute observation session after at least five minutes of habituation.

2.4 Electrophysiological assessments

Electrophysiological assessments were carried out in accordance with accepted practices [24, 25]. Mice were initially put to sleep with an intraperitoneal injection of 0.8% pentobarbital sodium using a BL-420F device with preset parameters to record signals. To access the sciatic nerve, a small incision was performed on the right hind limb after the skin had been shaved, prepared, and disinfected. Warm glycerin was used to lubricate the exposed nerve, and a heating lamp was used to keep the animal's body temperature stable and avoid cold extremities, which could impede nerve conduction. The gastrocnemius muscle served as the reference electrode, while the ankle, between the second and third toes of the hind limb, served as the recording electrode. Then, using rectangular pulses lasting 0.2 ms, a 1V voltage at a frequency of 0.10 Hz was used to activate the sciatic nerve. By dividing the distance (S) between the two recording electrodes by the difference in latency (Δt) between the recorded signals, sensory nerve conduction velocity (SNCV), expressed in meters per second (m/s), was computed: $V = S/\Delta t$.

2.5 Hematoxylin & eosin (H&E) staining

Tissue samples were preserved in 10% formalin after dissection and kept at 4 °C for the whole night. After that, they were sectioned into 4 μm thick slices, placed on a microtome, and embedded in paraffin. The parts were immersed in xylene I and II for 30 minutes each after being heated to 65°C for 30 minutes to dewax them. After that, a series of graded ethanol was used: 100% ethanol twice for ten minutes each, followed by 95% for five minutes, 85% for one minute, and 75% for one minute. The sections were stained with 200 μl of hematoxylin solution for 4 minutes at room temperature following a 5-minute PBS wash. After giving them a thorough rinse under running tap water from the back, they were treated with a distinguishing solution for eight minutes, washed in PBS for five minutes, and then rinsed under running water once more. After applying 400 μl of eosin solution for 30 seconds, there was one last rinse under running tap water. The samples were cleaned in xylene I and II for two minutes each after being dehydrated twice in 100% ethanol for one minute each. After applying cover slips, an Olympus light microscope (Tokyo, Japan) with a ×100 objective lens was used to analyze the histological alterations [26].

2.6 Silver stain

The tissue slices were first dewaxed by immersing them in xylene I and II for 20 minutes each, then absolute ethanol I and II for 5 minutes each, and finally 75% ethanol for 5 minutes. They were rinsed with distilled water, stained for five minutes with silver glycine staining solution C, and then rinsed three more times with distilled water. After that, silver glycine staining solution B was used for three to five minutes. The sections

were temporarily submerged in a preheated silver glycine staining solution (A I) for five seconds after the desired attenuation effect was observed. They were then promptly moved into solution (A II) for a further five seconds. They were dehydrated and rinsed after removal. The sections were dehydrated by submerging them for five minutes in each of three changes of 100% ethanol, followed by xylene I. A stop solution was used to prevent silver complexes from forming. Lastly, a microscope examination of the produced samples was conducted.

2.7 Transmission electron microscope analysis of sciatic nerve

Transmission electron microscopy (TEM) was conducted using the Zhang et al. (2019) methodology [27]. The mice were given an intraperitoneal injection of 0.8% sodium pentobarbital to induce anesthesia, and then they were perfused with regular saline. The sciatic nerves were embedded in epoxy resin after being treated in 10% paraformaldehyde for an entire night at 4°C. A solution comprising 0.4% uranyl acetate and 2% lead citrate was used to stain ultrathin sections that were 0.4 nm thick. A Hitachi (Tokyo, Japan) transmission electron microscope was then used to analyze these sections at magnifications of 2000 and 15,000 in order to look for morphological changes.

2.8 Immunofluorescence analysis

The paraffin sections were dewaxed by heating at 65°C for 30 minutes. They were then *immersed* in xylene I and II for 10 minutes each, followed by rehydration in a graded ethanol series: two changes of 100% ethanol for 6 minutes each, 95% for 3 minutes, 85% for 2 minutes, and 75% for 1 minute. After a 1-minute wash in PBS, antigen retrieval was performed by heating the sections in retrieval buffer at 85-100°C for 20 minutes. They were washed three times in PBST for 3 minutes each, excess liquid was removed, and the tissue was circled to contain subsequent reagents. The sections were treated with 0.1% Triton X-100 for 5 minutes, blotted, treated again with 0.1% Triton X-100 for 10 minutes, and washed three times in PBST for 3 minutes each. Endogenous peroxidase was blocked with an inhibitor for 10 minutes, followed by another three PBST washes. After blocking with 3% BSA for 30 minutes and three more PBST washes, the sections were incubated overnight at 4°C with a primary antibody: mouse anti-p-NF-κB p65 antibody (1:200 dilution). Following three PBST washes and removal of excess liquid, the sections were incubated in the dark at 4°C for 1 hour with a fluorescein (FITC)-conjugated goat anti-rabbit secondary antibody (1:200 dilution). After three final PBST washes, nuclei were stained with DAPI for 5-10 minutes in the dark, followed by three more PBST washes. A spontaneous fluorescence quenching reagent was applied for 5 minutes before mounting coverslips for observation.

2.9 Elisa

Spinal cord tissues were homogenized on ice in pre-chilled 0.01M PBS (pH 7.4) containing a protease inhibitor. The homogenate was centrifuged at 10,000 × g for 10 minutes at 4°C, after which the supernatant was collected. The concentrations of IL-1β, IL-6, and TNF-α

in the supernatant were measured using specific ELISA kits (Bioswamp Company, China; Batch Nos. MU30369, MU30044, and MU30030, respectively), following the manufacturer's protocols.

2.10 Quantitative PCR

Spinal cord tissues were harvested and homogenized. Total RNA was isolated using Trizol reagent, followed by reverse transcription with TransScript Uni-in-one (Transgen, China; Batch No. AU341). Primer sequences (see Table 1) were designed using the online Primer-BLAST tool (https://www.ncbi.nlm.nih.gov/tools/primer-blast/). Quantitative PCR (qPCR) was subsequently performed with PerfectStart reagents (Transgen, China; Batch No. AQ601) in accordance with the manufacturer's protocol.

2.11 Statistical analysis

Statistical analysis was performed with SPSS 25.0 and GraphPad Prism 8.02 software. Data are presented as mean ± standard deviation ($\bar{X} \pm S$). A one-way analysis of variance (ANOVA) was used to assess the effects of BDCM on protein expression levels. For comparisons between two sample means, a two-way repeated measures ANOVA with post-hoc testing was applied. A $P < 0.05$ value was considered statistically significant.

3. Results

3.1 Effects of BDCM on PWT in VCR-induced NP mice

The influence of BDCM on PWT is shown in Figure 2a over the subsequent 11 days, the PWT of the VCR + NS model group remained significantly lower compared to the normal control group ($P < 0.01$). By day 16 and day 21, the PWT in the VCR + BDCM (80 mg/kg) and VCR + pregabalin groups was significantly greater than in the VCR + NS model group ($P < 0.01$). Furthermore, a significant increase in PWT was observed on day 21 in the VCR + BDCM (40 mg/kg) group compared to the model group ($P < 0.05$). However, no significant change in PWT was noted between day 11 and day 21 in the VCR + BDCM (20 mg/kg) group ($P > 0.05$).

3.2 Effects of BDCM on PWL in VCR-induced NP mice

In the thermal radiation test, as shown in Figure 2b, the VCR + NS model group showed a significant decrease in PWL ($P < 0.01$) compared to the normal control group. On days 16 and 21, when comparing the VCR + NS model group to both the VCR + BDCM (80 mg/kg) and VCR + Pregabalin groups, PWL was significantly greater in the latter two groups ($P < 0.01$). Additionally, by day 21, administration of VCR+ BDCM at a dosage of 40 mg/kg resulted in a significant increase in PWL compared to baseline ($P < 0.05$). However, no significant difference in PWL was observed between days 11 and 21 in the group treated with VCR + BDCM at 20 mg/kg ($P > 0.05$).

3.3 Effects of BDCM on the number of paw lifts in VCR-induced NP mice

The effects of BDCM on the number of paw lifts, as shown in Figure 2c. In the VCR + NS model group, the number of paw lifts significantly increased ($P < 0.05$) initially, followed by a significant decrease by day 7. In comparison, the VCR + Pregabalin group exhibited a significant decrease in paw lifts compared to the VCR + NS group ($P < 0.01$). For the VCR + BDCM groups, the 20 mg/kg dosage did not show a significant difference in paw lifts ($P > 0.05$). However, the VCR + BDCM (80 mg/kg) and VCR + BDCM (40 mg/kg) groups both showed a significant decrease in paw lifts ($P< 0.05$ and $P < 0.01$, respectively).

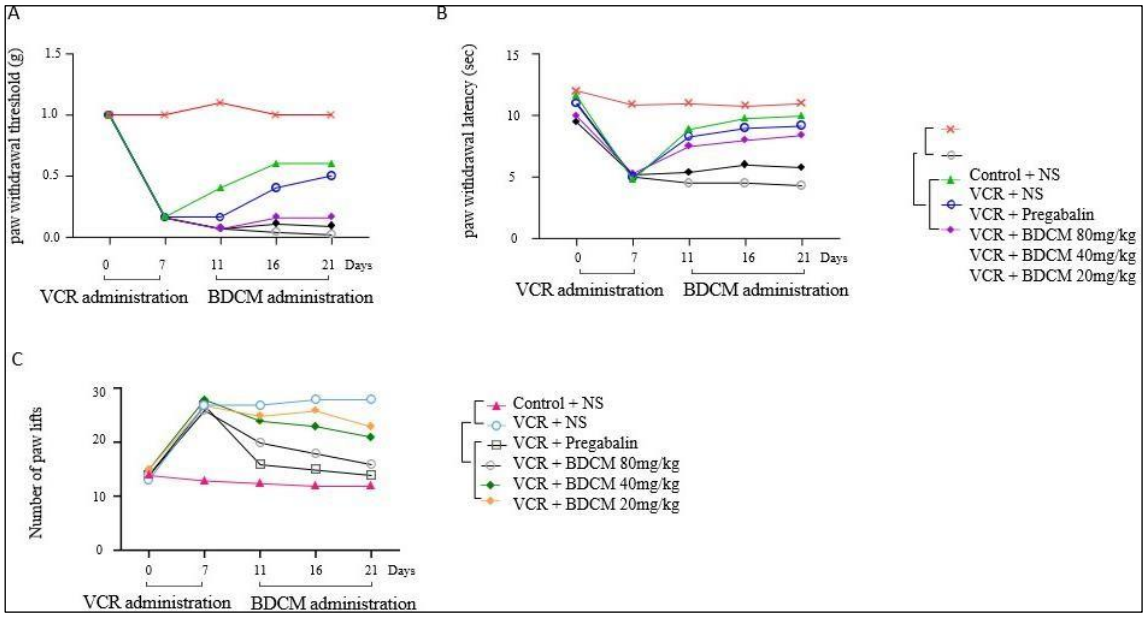

Figure 2: Effects of BDCM on behavioral tests. (a) The Von Frey filament test was used to assess the effects of BDCM on PWT in VCR induced NP mice models. (b) Effects of BDCM on PWL by thermal radiation. (c) The effects of BDCM on the number of paw lifts in VCR induced NP mice models. ($\bar{X} \pm S$, n=10); Compared to the control group: $^{*}P < 0.05$, $^{**}P < 0.05$, compared to the VCR group: $^{\#}P < 0.05$, $^{\#\#}P < 0.01$.

3.4 Effects of BDCM on SNCV in VCR-induced NP mice

The results of the electrophysiology test on SNCV are shown in Figure 3. In the VCR + NS group, the amplitudes of action potentials were significantly reduced, and the latency was notably prolonged compared to the Control + NS group.

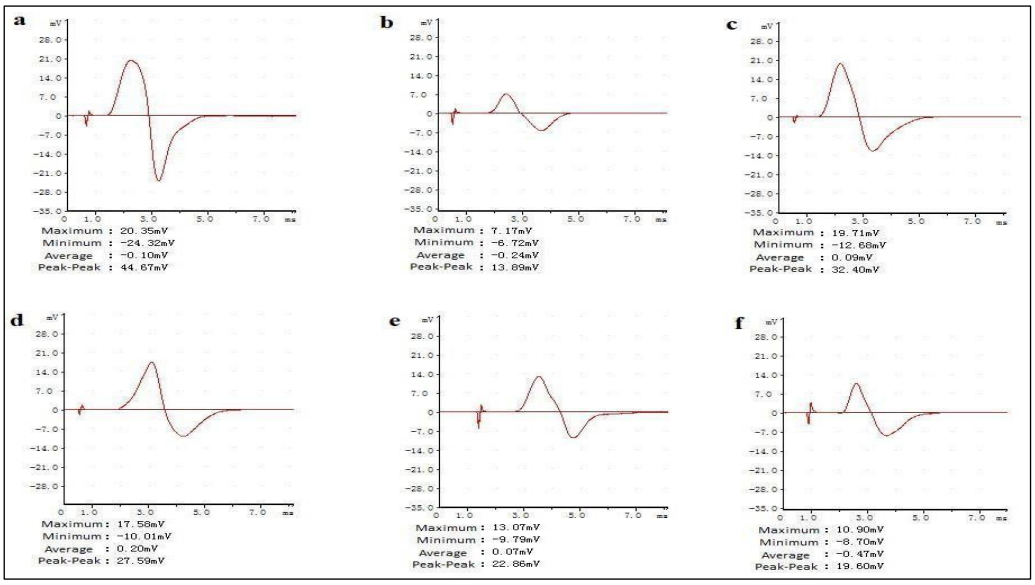

Figure 3: The effects of BDCM on compound action potential (CAP) in the sciatic nerve of mice. (a) CAP traces of the control group, (b**)** CAP traces of the VCR group, (c**)** CAP traces of the VCR + Pregabalin group. (d, e, f**)** CAP traces of VCR + BDCM **(**80, 40, 20 kg/mg) respectively

Additionally, the SNCV in the VCR + NS group was significantly lower ($P < 0.01$) than that in the Control + NS group. After 10 days of treatment, the SNCV in the VCR + BDCM (40 mg/kg, 80 mg/kg) and VCR + Pregabalin (10 mg/kg) groups showed a significant increase ($P < 0.05$) compared to the VCR + NS group.

3.5 Effects of BDCM on H&E staining of sciatic nerves in VCR-induced NP mice

H&E staining was performed to assess the pathological changes in the sciatic nerve following BDCM treatment (Figure 4). In the VCR + NS group, compared to the Control + NS group, significant alterations were observed, including disruption of axon alignment, myelin sheath degradation, and the presence of distinct gaps and empty spaces between cells. In contrast, the VCR + BDCM group showed notable improvements in sciatic nerve morphology, with better alignment of axons and myelin sheaths, as compared to both the VCR + NS group and the VCR + pregabalin group (at both 40 mg/kg and 80 mg/kg doses).

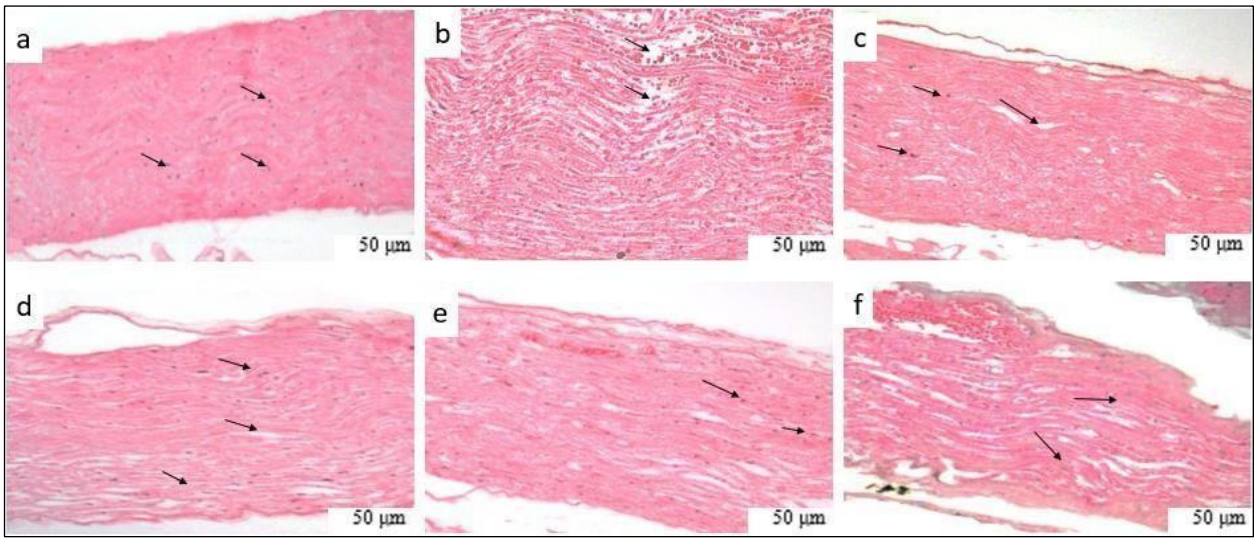

Figure 4: Microscopic observation of hematoxylin and eosin-stained sections of sciatic nerves. (a) An image from the Control group presenting multiple axons (arrowheads). (b) VCR group showing several lost axons (arrowheads) with lost myelin sheaths. (c) VCR+Pregabalin group shows improved neuronal axons (arrowheads). (d, e, f**)** traces of VCR + BDCM **(**80, 40, 20 kg/mg) respectively, showing an increased number of axons (arrowheads) compared to the VCR group. (Scale bar= 50 µm)

3.6 Effects of BDCM on silver staining of sciatic nerves in VCR-induced NP mice

Silver staining was used to study the structural abnormalities in the sciatic nerve induced by VCR. In the VCR + NS group, significant disruptions in the orientation of nerve fiber axons were evident, characterized by a dark silver stain, compared to the Control + NS group as shown in Figure 5. Conversely, the VCR + BDCM (80mg/kg) group showed improved alignment of nerve fiber axons, with a less intense silver stain relative to both the VCR + NS group and the VCR + pregabalin group (at a dose of 10 mg/kg).

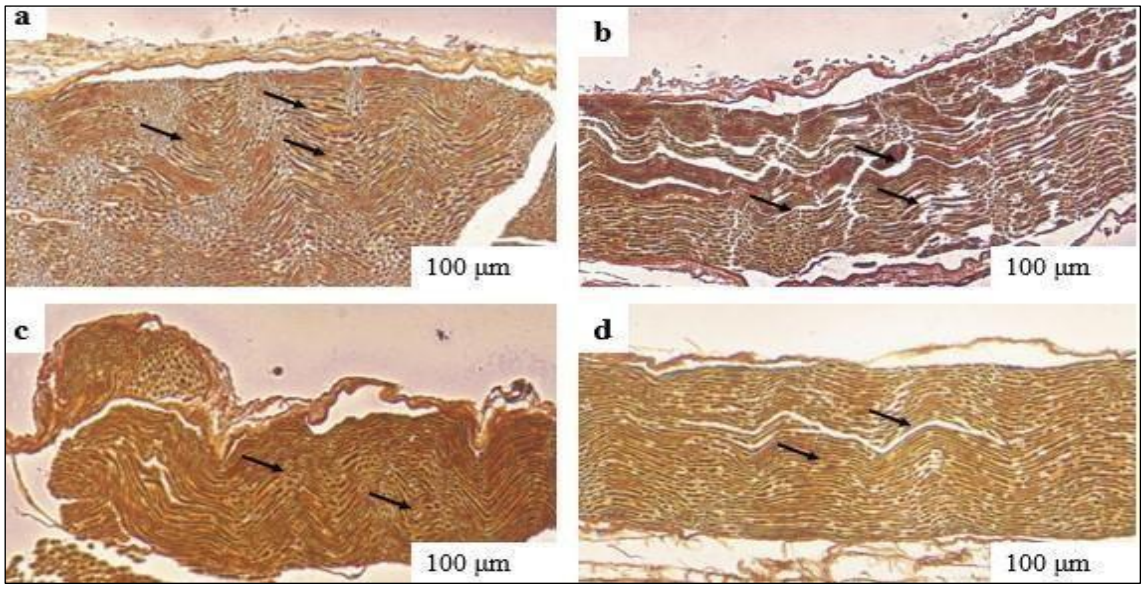

Figure 5: Effects of BDCM on silver staining of sciatic nerve specimens in VCR-induced neuropathic pain. Images show well-organized nerve fiber axons in the (a) control + NS group, intense staining by silver stain, and a substantial disorganized nerve fiber axon pattern in the (b) VCR+NS group, less degeneration in the nerve fiber axons, and reduced silver staining in the (c**)** VCR + pregabalin and **(**d) VCR+BDCM 80mg/kg groups respectively. (Scale bar= 100 µm)

3.7 Effects of BDCM on TEM analysis of sciatic nerves in VCR-induced NP mice

The findings of the transmission electron microscope indicated that the myelin sheaths of the Control + NS group showed a dense, transparent, and oval appearance. The findings in the VCR + NS group revealed the presence of deteriorated myelinated axons (*Figure.6-7*). Following the administration of pregabalin and BDCM, the myelin sheath of the pregabalin group (10mg/kg) and the BDCM group (80mg/kg) showed significant improvement; the myelin sheathes and axons in both groups seemed regular and well-formed.

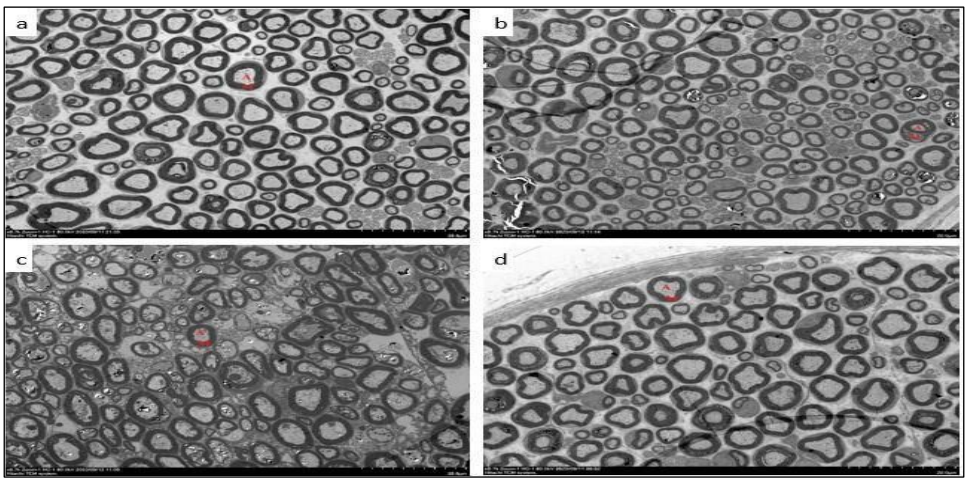

Figure 6: The effect of BDCM on ultrastructural changes in the sciatic nerve of VCR-induced neuropathic pain mice observed by TEM. (a) Control + NS; (b): VCR+NS; (c): VCR + Pregabalin; (d): VCR+BDCM 80mg/kg. (Scale bar= 20 µm).

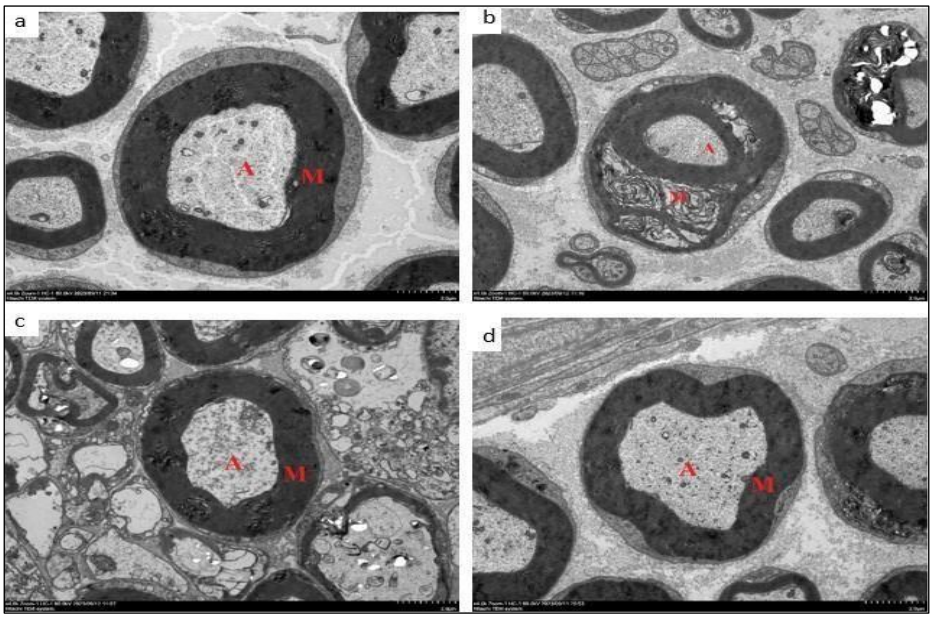

Figure 7: Observation of the effect of BDCM on ultrastructural changes in the sciatic nerve of VCR-induced neuropathic pain mice by TEM. (A: axons, M: myelin sheath, scale bar= 2 μm) (a) Control + NS; showing the normal characteristics of myelinated axons with regular myelin sheaths. (b) VCR+NS; showing degenerated myelinated axons. (c, d) VCR + Pregabalin, VCR+BDCM 80mg/kg; Treated groups showed myelinated axons with regular myelin sheaths, respectively

3.8 Effects of BDCM on p-NF-κB p65 expression levels in spinal Cord

The expression levels of p-NF-κB p65 were observed in the spinal cord by a green immunostain (*Figure 8*). Compared with the Control + NS group, the expression levels of p-NF-κB p65 in the VCR + NS group increased significantly ($P < 0.01$). Compared with the VCR + NS group, the expression of p-NF-κBp65 in the VCR + Pregabalin 10 mg/kg and VCR + BDCM 80 mg/kg groups decreased significantly.

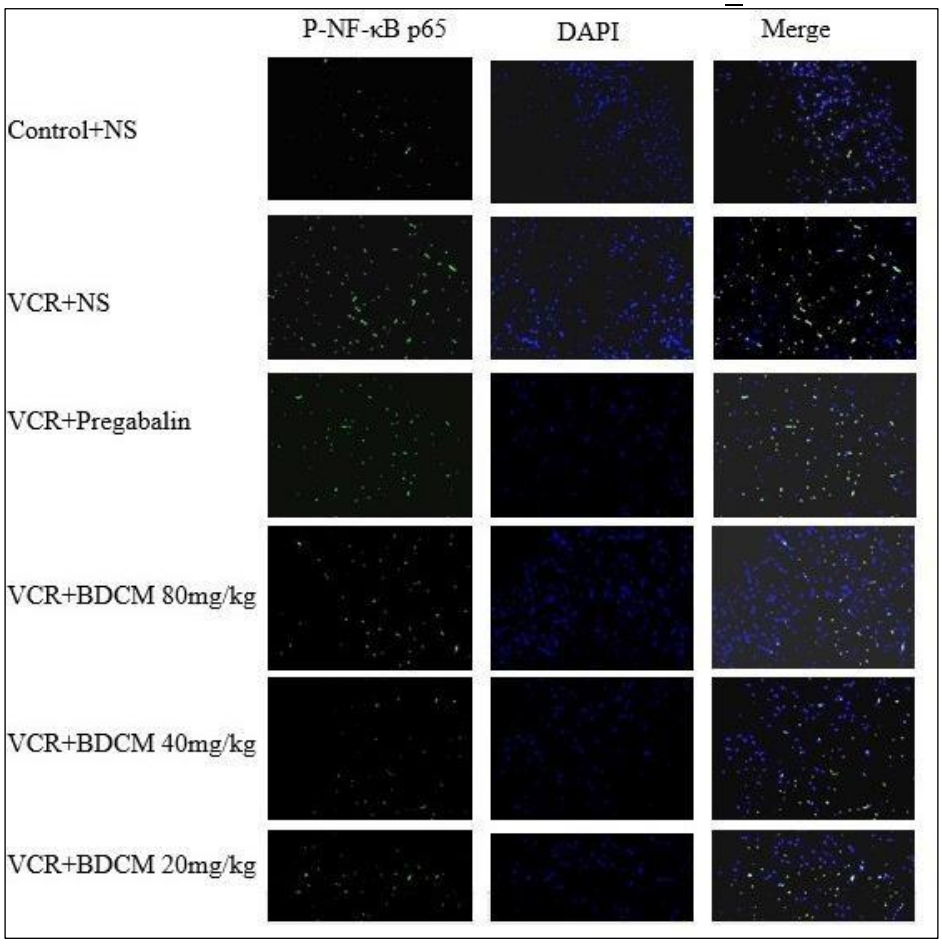

Figure 8: Effects of BDCM on p-NF-κB p65 expression in the spinal cord. ($\bar{X} \pm S$, n=5) Compared to the control group, the VCR group showed increased expression levels of p-NF-κB p65. While in the Pregabalin and BDCM (20, 40, 80mg/kg) treatment groups, decreased levels of on p-NF-κB p65 were observed (Scale bar= 450 μm).

3.9 Effects of BDCM on pro-inflammatory cytokine expression

The protective effects of BDCM were assessed by its ability to suppress the expression levels of pro-inflammatory cytokines through ELISA and Q-PCR analysis. As shown in *Figure. 9*, ELISA results showed a significant increase in the levels of IL-1β, IL-6, and TNF-α in the tissues of the VCR + NS group compared to those in the Control + NS ($p < 0.01$). While BDCM (80 mg/kg) significantly decreased the expression of IL-1β, IL-6, and TNF-α levels. A similar phenomenon was observed in the Q-PCR results *Figure. 10*, the levels of IL-1β, IL-6, and TNF-α mRNA were highly expressed in the VCR + NS group compared to those in the Control + NS ($p < 0.01$). And the BDCM (80 mg/kg) suppressed the expression of IL-1β, IL-6, and TNF-α mRNA levels.

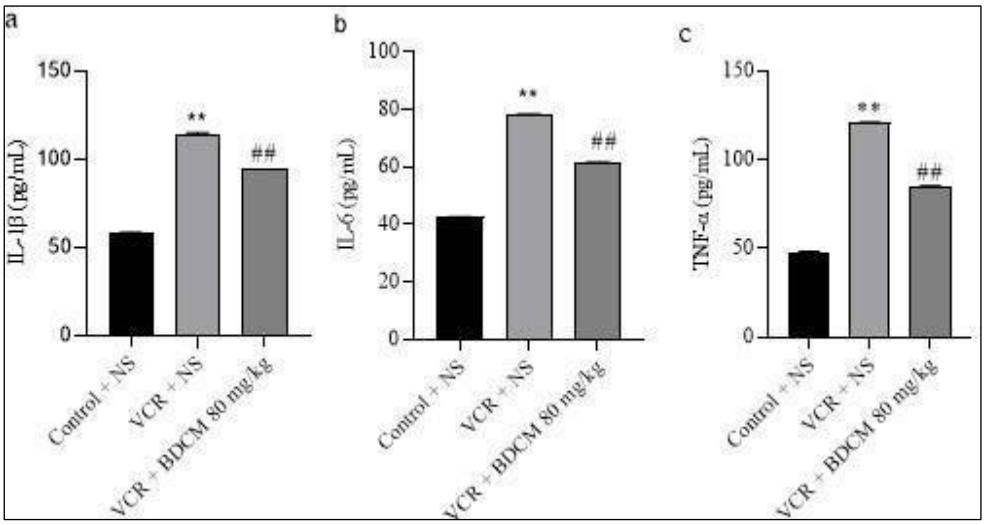

Figure 9: Effect of BDCM on pro-inflammatory cytokine expression as observed by ELISA (a) IL-1β, (b) IL-6, and (c) TNF-α (pg/mL) expression in the spinal cord of mice ($\bar{X}$ ±, n=6). Compared with the control group: $^{**}P < 0.01$; Compared with the VCR group: $^{\#\#}P < 0.05$

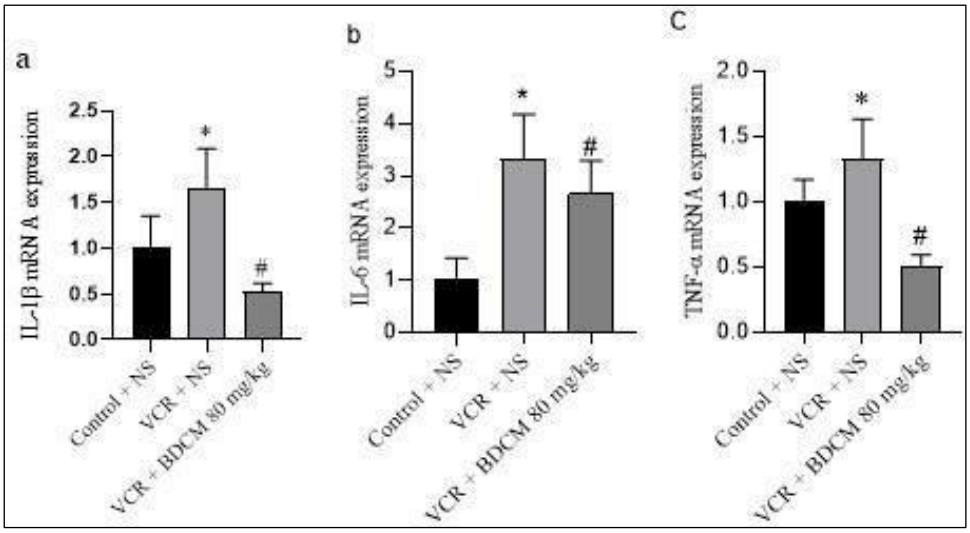

Figure 10: Effect of BDCM on mRNA expression as observed by PCR (a) IL-1β, (b) IL-6, and (c) TNF-α mRNA expression in the spinal dorsal horn of mice ($\bar{X}$ ±, n=6). Compared with the control group: $^{*}P < 0.05$; Compared with the VCR group: $^{\#}p < 0.05$.

4. Discussion

One common side effect of chemotherapy is neuropathic pain, which is caused by damage to the somatosensory nerve system [28]. This serious and long-lasting side effect can interfere with treatment plans and reduce the effectiveness of anticancer medications. Even after therapy is over, about 68% of patients retain this pain, and one in three report persistent, chronic discomfort [29]. As a result, pharmaceutical research has made creating low-toxicity, less addictive analgesics from natural sources a top focus. Curcuma longa contains a bioactive molecule called bisdemethoxycurcumin (BDCM), which has been shown to have anti-inflammatory, antioxidant, and anticancer properties [30, 31].

NF-κB, a transcription factor, controls processes such as inflammation, pain signaling, immune response, and cell growth and differentiation [32, 33]. It plays a key role in releasing pro-inflammatory substances like TNF-α and IL-6, which are involved in both the onset and sustenance of neuropathic pain (*Figure 11*). Nerve injury can activate NF-κB, which then contributes to pain development [34]. Our results indicated increased NF-κB p65 expression in the spinal cord after vincristine (VCR) treatment. This suggests that the rise in NF-κB p65 following spinal cord injury may activate spinal neurons and increase both NF-κB p65 mRNA and protein. In contrast, oral administration of BDCM reduced NF-κB p65 levels in mice with chemotherapy-induced neuropathic pain (CINP).

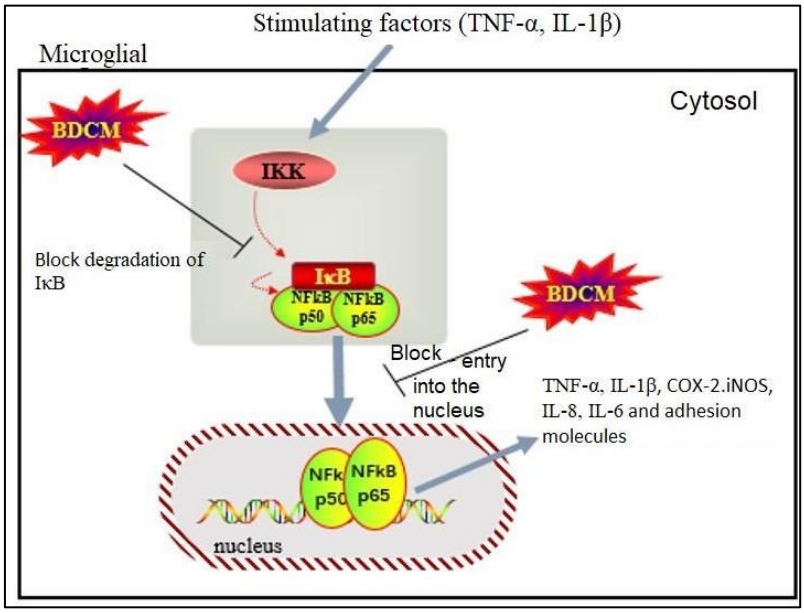

Figure 11: Mechanism of NF-κB activation. The activation of NF-κB has been reported to induce transcription of multiple pro-inflammatory cytokines and pivotal enzymes that are involved in maintaining inflammation such as TNF-α, IL-1β, IL-6 and others. Therefore, inhibiting NF-κB activation could attenuate inflammation

The study assessed the pain-relieving potential of BDCM and measured pain sensitivity using von Frey filaments. The results showed that whereas the PWT in the VCR + NS group dropped by more than 60%, mice in the control + NS group maintained a steady PWT throughout the testing period. Increased PWT was seen in mice treated with VCR + BDCM, indicating that BDCM, like pregabalin, significantly reduces mechanical hypersensitivity in mice with VCR-induced neuropathic pain. The cold plate test was used to assess cold pain sensitivity, and the results showed a considerable reduction in the number of foot withdrawals. Foot withdrawals were more common in the VCR + BDCM and VCR + pregabalin groups, suggesting that BDCM and pregabalin can lessen hypersensitivity to cold pain in this model. Additionally, a radiant heat stimulation was used to test for thermal hyperalgesia, which showed a significant decrease in PWL. In mice with VCR-induced neuropathic pain, the study found that both BDCM and pregabalin significantly improved thermal hyperalgesia.

Hematoxylin and eosin (H&E) staining was used in the study to examine pathological alterations in the sciatic nerve of mice experiencing neuropathic pain. The control + NS group's tissue architectures were found to be normal. The VCR + BDCM and VCR + pregabalin groups, on the other hand, showed indications of regeneration, such as repaired myelin sheaths and neuronal axons. These staining results show that BDCM and pregabalin may both alleviate sciatic nerve damage, suggesting a possible neuroprotective function through nerve healing. Additionally, TEM and silver staining were used to evaluate the neuroprotective impact of BDCM on sciatic nerve injury caused by vincristine. The results showed that both BDCM (80 mg/kg) and pregabalin (10 mg/kg) encouraged the restoration of normal sciatic nerve structure, indicating that BDCM treatment may lessen nerve damage brought on by VCR. Additionally, Analysis by Q-PCR and ELISA revealed that mRNA and protein levels of NF-κB p65, TNF-α, IL-1β, and IL-6 in the spinal dorsal horn were markedly higher in the VCR + NS group than in the control+ NS group. In contrast, these levels were significantly lower in the VCR + BDCM group. This indicates that BDCM alleviates VCR-induced neuropathic pain by inhibiting the activation of the NF-κB signaling
pathway in the spinal cord.

In conclusion, BDCM has potential as a treatment for attenuating behavioral symptoms and protecting the sciatic nerve from damage induced by VCR-induced neuropathic pain. However, more research is needed to thoroughly examine its molecular mechanisms and uncover potential treatment targets. In order to thoroughly explore possible targets of BDCM in the treatment of neuropathic pain, network pharmacology might be useful.

Funding Statement
Not applicable.

Acknowledgments
The figures and schemes presented in this article are original and have not been copied or adapted from any other sources.

Authorship Contributions
The author C.M; designed the article outline, literature review, experimental research, data analysis and wrote the manuscript. Was responsible for statistical analysis. Contributed to manuscript editing and review. The author approved the final manuscript.

Availability of Data
The data that support the findings of this study are available from the corresponding author upon reasonable request. Some data may not be made available because of privacy or ethical restrictions.

Consent for Publication
Not applicable.

Ethics Declarations
All animal experiments were performed in accordance with the National Institutes of Health Guidelines for the Care and Use of Laboratory Animals and approved by the Ethics Committee of The Ningxia Medical University.

Abbreviations
NP - neuropathic pain,
CINP - chemotherapy-induced neuropathic pain
BDCM - bisdemethoxycurcumin,
VCR - vincristine,
TEM - transmission electron microscopy,
NF-κB - nuclear factor kappa B,
PWL - paw withdrawal latency,
PWT - paw withdrawal threshold.

Conflict of Interest Statement
The author declares no conflicts of interest.

About the Author(s)
Chalton Manengu is a PhD student focusing on mechanisms that induce heart failure. His other research interests include neuropathic pain evaluation.
Research Gate: https://www.researchgate.net/profile/Chalton-Manengu-2

References

1) D'Souza RS, Alvarez GAM, Dombovy-Johnson M, Eller J, Abd-Elsayed A. Evidence-Based Treatment of Pain in Chemotherapy-Induced Peripheral Neuropathy. Current pain and headache reports. 2023;27(5):99-116. https://doi.org/10.1007/s11916-023-01107-4
2) Sisignano M, Baron R, Scholich K, Geisslinger G. Mechanism-based treatment for chemotherapy-induced peripheral neuropathic pain. Nature Reviews Neurology. 2014;10(12):694-707. https://doi.org/10.1038/nrneurol.2014.211
3) Zhang S. Chemotherapy-induced peripheral neuropathy and rehabilitation: A review. Seminars in oncology. 2021;48(3):193-207. https://doi.org/10.1053/j.seminoncol.2021.09.004
4) Bae EH, Greenwald MK, Schwartz AG. Chemotherapy-Induced Peripheral Neuropathy: Mechanisms and Therapeutic Avenues. Neurotherapeutics: the journal of the American Society for Experimental Neuro Therapeutics. 2021;18(4):2384-96. https://doi.org/10.1007/s13311-021-01142-2
5) Bennett GJ, Doyle T, Salvemini D. Mitotoxicity in distal symmetrical sensory peripheral neuropathies. Nature Reviews Neurology. 2014;10(6):326-36. https://doi.org/10.1038/nrneurol.2014.77
6) Liu T, Zhang L, Joo D, Sun SC. NF-κB signaling in inflammation. Signal transduction and targeted therapy. 2017;2:17023. https://doi.org/10.1038/sigtrans.2017.23
7) Singh S, Singh TG. Role of Nuclear Factor Kappa B (NF-κB) Signalling in Neurodegenerative Diseases: A Mechanistic Approach. Current neuropharmacology. 2020;18(10):918-35. https://doi.org/10.2174/1570159x18666200207120949
8) Guo HM, Zhang Y, Zhang Y, Jiao PF, Fan XC, Kong CL, et al. Spinal Ninjurin2 contributes to the neuropathic pain via NF-κB-mediated neuroinflammation in the spared sciatic nerve injury rats. International immunopharmacology. 2021;99:107918. https://doi.org/10.1016/j.intimp.2021.107918
9) Lee KM, Kang BS, Lee HL, Son SJ, Hwang SH, Kim DS, et al. Spinal NF-kB activation induces COX-2 upregulation and contributes to inflammatory pain hypersensitivity. The European journal of neuroscience. 2004;19(12):3375-81. https://doi.org/10.1111/j.0953-816X.2004.03441.x
10) Ahmed AS, Berg S, Alkass K, Druid H, Hart DA, Svensson CI, et al. NF-κB-Associated Pain-Related Neuropeptide Expression in Patients with Degenerative Disc Disease. International journal of molecular sciences. 2019;20(3). https://doi.org/10.3390/ijms20030658
11) Kunnumakkara AB, Shabnam B, Girisa S, Harsha C, Banik K, Devi TB, et al. Inflammation, NF-κB, and Chronic Diseases: How are They Linked? Critical reviews in immunology. 2020;40(1):1-39. https://doi.org/10.1615/CritRevImmunol.2020033210

12) Roberti A, Chaffey LE, Greaves DR. NF-κB Signaling and Inflammation-Drug Repurposing to Treat Inflammatory Disorders? Biology. 2022;11(3). https://doi.org/10.3390/biology11030372
13) Huang C, Lu HF, Chen YH, Chen JC, Chou WH, Huang HC. Curcumin, demethoxycurcumin, and bisdemethoxycurcumin induced caspase-dependent and -independent apoptosis via Smad or Akt signaling pathways in HOS cells. BMC complementary medicine and therapies. 2020;20(1):68. https://doi.org/10.1186/s12906-020-2857-1
14) Wang Q, Liu J, Liu J, Thant YM, Weng W, Wei C, et al. Bisdemethoxycurcumin-conjugated vitamin E TPGS liposomes ameliorate poor bioavailability of free form and evaluation of its analgesic and hypouricemic activity in oxonate-treated rats. 2021;23.
15) Jin G, Xu W, Tang H, Cui Y, Zhang H. Bisdemethoxycurcumin, a curcumin, protects chondrocytes, and reduces cartilage inflammation via the NRF2/HO-1/NLRP3 pathway. Immunity, inflammation and disease.2024;12(2):e1195. https://doi.org/10.1002/iid3.1195
16) Sun X, Liang Y, Wang Y, Sun C, Wang X. Bisdemethoxycurcumin, a curcumin derivative, ameliorates adjuvant-induced arthritis by suppressing inflammatory reactions and macrophage migration. Chemico-biological interactions. 2024;387:110822. https://doi.org/10.1016/j.cbi.2023.110822
17) Guo, Cai XF, Lee JJ, Kang SS, Shin EM, Zhou HY, et al. Comparison of suppressive effects of demethoxycurcumin and bisdemethoxycurcumin on expressions of inflammatory mediators in vitro and in vivo. Archives of pharmacal research. 2008;31(4):490-6. https://doi.org/10.1007/s12272-001-1183-8
18) Authier N, Gillet JP, Fialip J, Eschalier A, Coudore F. A new animal model of vincristine-induced nociceptive peripheral neuropathy. Neurotoxicology. 2003;24(6):797-805. https://doi.org/10.1016/s0161-813x(03)00043-3
19) Sweitzer SM, Pahl JL, DeLeo JA. Propentofylline attenuates vincristine-induced peripheral neuropathy in the rat. Neuroscience letters. 2006;400(3):258-61. https://doi.org/10.1016/j.neulet.2006.02.058
20) Chaplan SR, Bach FW, Pogrel JW, Chung JM, Yaksh TL. Quantitative assessment of tactile allodynia in the rat paw. Journal of neuroscience methods. 1994;53(1):55-63. https://doi.org/10.1016/0165-0270(94)90144-9
21) Hargreaves K, Dubner R, Brown F, Flores C, Joris J. A new and sensitive method for measuring thermal nociception in cutaneous hyperalgesia. Pain. 1988;32(1):77-88. https://doi.org/10.1016/0304-3959(88)90026-7
22) Cheah M, Fawcett JW, Andrews MR. Assessment of Thermal Pain Sensation in Rats and Mice Using the Hargreaves Test. Bio-protocol. 2017;7(16). https://doi.org/10.21769/BioProtoc.2506
23) Jasmin L, Kohan L, Franssen M, Janni G, Goff JR. The cold plate as a test of nociceptive behaviors: description and application to the study of chronic

neuropathic and inflammatory pain models. Pain. 1998;75(2-3):367-82. https://doi.org/10.1016/s0304-3959(98)00017-7

24) Chiechio S, Copani A, Gereau RWt, Nicoletti F. Acetyl-L-carnitine in neuropathic pain: experimental data. CNS drugs. 2007;21 Suppl 1:31-8; discussion 45-6. https://doi.org/10.2165/00023210-200721001-00005
25) Gabay E, Tal M. Pain behavior and nerve electrophysiology in the CCI model of neuropathic pain. Pain. 2004;110(1-2):354-60. https://doi.org/10.1016/j.pain.2004.04.021
26) Sudoh Y, Desai S, Haderer AE, Sudoh S, Gerner P, Anthony DC, et al. Neurologic and histopathologic evaluation after high-volume intrathecal amitriptyline. 2004;29:434 - 40.
27) Zhang., Liu N, Zhu C, Ma L, Yang J, Du J, et al. Antinociceptive effect of isoorientin against neuropathic pain induced by the chronic constriction injury of the sciatic nerve in mice. International immunopharmacology. 2019;75:105753. https://doi.org/10.1016/j.intimp.2019.105753
28) Staff NP, Grisold A, Grisold W, Windebank AJ. Chemotherapy-induced peripheral neuropathy: A current review. Annals of neurology. 2017;81(6):772-81. https://doi.org/10.1002/ana.24951
29) Seretny M, Currie GL, Sena ES, Ramnarine S, Grant R, MacLeod MR, et al. Incidence, prevalence, and predictors of chemotherapy-induced peripheral neuropathy: A systematic review and meta-analysis. Pain. 2014;155(12):2461-70. https://doi.org/10.1016/j.pain.2014.09.020
30) Araújo CC, Leon LL. Biological activities of Curcuma longa L. Memorias do Instituto Oswaldo Cruz. 2001;96(5):723-8. https://doi.org/10.1590/s0074-02762001000500026
31) Wakte PS, Sachin BS, Patil AA, Mohato DM, Band TH, Shinde DJS, et al. Optimization of microwave, ultra-sonic and supercritical carbon dioxide assisted extraction techniques for curcumin from Curcuma longa. 2011;79:50-5.
32) Kaltschmidt C, Greiner JFW, Kaltschmidt B. The Transcription Factor NF-κB in Stem Cells and Development. Cells. 2021;10(8). https://doi.org/10.3390/cells10082042
33) Oeckinghaus A, Ghosh S. The NF-kappaB family of transcription factors and its regulation. Cold Spring Harbor perspectives in biology. 2009;1(4):a000034. https://doi.org/10.1101/cshperspect.a000034
34) Yin Q, Fan Q, Zhao Y, Cheng MY, Liu H, Li J, et al. Spinal NF-κB and chemokine ligand 5 expression during spinal glial cell activation in a neuropathic pain model. PLoS One. 2015;10(1):e0115120. https://doi.org/10.1371/journal.pone.0115120

Appendix: Figure Captions

Figure 1: Chemical structure of Bisdemethoxycurcumin (BDCM).

Figure 2: Effects of BDCM on behavioral tests. (a) The Von Frey filament test was used to assess the effects of BDCM on PWT in VCR induced NP mice models. (b) Effects of BDCM on PWL by thermal radiation. (c) The effects of BDCM on the number of paw lifts in VCR induced NP mice models. ($X \pm S$, n=10); Compared to the control group: $^{*}P < 0.05$, $^{**}P < 0.05$, compared to the VCR group: $^{\#}$ P < 0.05, $^{\#\#}P < 0.01$.

Figure 3: The effects of BDCM on compound action potential (CAP) in the sciatic nerve of mice. (a) CAP traces of the control group, (b**)** CAP traces of the VCR group, (c**)** CAP traces of the VCR + Pregabalin group. (d, e, f**)** CAP traces of VCR + BDCM **(**80, 40, 20 kg/mg) respectively.

Figure 4: Microscopic observation of hematoxylin and eosin-stained sections of sciatic nerves. (a) An image from the Control group presenting multiple axons (arrowheads). (b) VCR group showing several lost axons (arrowheads) with lost myelin sheaths. (c) VCR+Pregabalin group shows improved neuronal axons (arrowheads). (d, e, f**)** traces of VCR + BDCM **(**80, 40, 20 kg/mg) respectively, showing an increased number of axons (arrowheads) compared to the VCR group. (Scale bar= 50 μm).

Figure 5: Effects of BDCM on silver staining of sciatic nerve specimens in VCR-induced neuropathic pain. Images show well-organized nerve fiber axons in the (a) control + NS group, intense staining by silver stain, and a substantial disorganized nerve fiber axon pattern in the (b) VCR+NS group, less degeneration in the nerve fiber axons, and reduced silver staining in the (c**)** VCR + pregabalin and **(**d) VCR+BDCM 80mg/kg groups respectively. (Scale bar= 100 μm).

Figure 6: The effect of BDCM on ultrastructural changes in the sciatic nerve of VCR-induced neuropathic pain mice observed by TEM. (a) Control + NS; (b): VCR+NS; (c): VCR + Pregabalin; (d): VCR+BDCM 80mg/kg. (Scale bar= 20 μm).

Figure 7: Observation of the effect of BDCM on ultrastructural changes in the sciatic nerve of VCR-induced neuropathic pain mice by TEM. (A: axons, M: myelin sheath, scale bar= 2 μm) (a) Control + NS; showing the normal characteristics of myelinated axons with regular myelin sheaths. (b) VCR+NS; showing degenerated myelinated axons. (c, d) VCR + Pregabalin, VCR+BDCM 80mg/kg; Treated groups showed myelinated axons with regular myelin sheaths, respectively.

Figure 8: Effects of BDCM on p-NF-κB p65 expression in the spinal cord. ($X \pm S$, n=5) Compared to the control group, the VCR group showed increased expression levels of p-

NF-κB p65. While in the Pregabalin and BDCM (20, 40, 80mg/kg) treatment groups, decreased levels of on p-NF-κB p65 were observed (Scale bar= 450 μm).

Figure 9: Effect of BDCM on pro-inflammatory cytokine expression as observed by ELISA (a) IL-1β, (b) IL-6, and (c) TNF-α (pg/mL) expression in the spinal cord of mice ($X \pm S$, n=6). Compared with the control group:
$^{**}P < 0.01$; Compared with the VCR group: $^{\#\#}P < 0.05$.

Figure 10: Effect of BDCM on mRNA expression as observed by PCR (a) IL-1β, (b) IL-6, and (c) TNF-α mRNA expression in the spinal dorsal horn of mice ($X \pm S$, n=6). Compared with the control group: $^{*}P < 0.05$; Compared with the VCR group: $^{\#}p < 0.05$.

Figure 11: Mechanism of NF-κB activation. The activation of NF-κB has been reported to induce transcription of multiple pro-inflammatory cytokines and pivotal enzymes that are involved in maintaining inflammation such as TNF-α, IL-1β, IL-6 and others. Therefore, inhibiting NF-κB activation could attenuate inflammation.

Table 1: The primer sequences used

Gene		Sequences
IL-1β	Forward primer Reverse primer	5′-ATC CCA AGC AAT ACC CAA AG-3′ 5′-GTG CTG ATG TAC CAG TTG GG-3′
IL-6	Forward primer Reverse primer	5′-GGA CCA AGA CCA TCC AAT TC-3′ 5′-ACC ACA GTG AGG AAT GTC CA-3.′
TNF-α	Forward primer Reverse primer	5′-ATG AGA AGT TCC CAA ATG GC-3′ 5′-CTC CAC TTG GTG GTT TGC TA-3′
GAPDH	Forward primer Reverse primer	5′-GGT TGT CTC CTG CGA CTT CA-3′ 5′-TGG TCC AGG GTT TCT TAC TCC-3′